Multi-wavelength Emission Signatures of Erupting Magnetic Flux Ropes

Anshika Singh[1], Bin Chen[1], Xiaocan Li[2], Joel Dahlin[3]

1. New Jersey Institute of Technology; 2. Los Alamos National Laboratory; 3. NASA Goddard Space Flight Center

Introduction

Coronal mass ejections (CMEs) driven by erupting magnetic flux ropes (MFRs) can cause significant geomagnetic storms and other space weather activity.

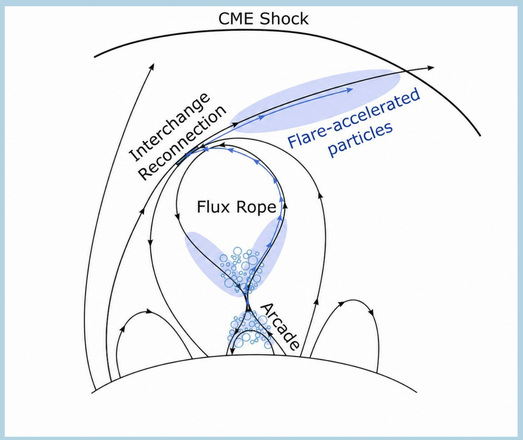


Figure 1. Schematic of an erupting magnetic flux rope and associated particle acceleration sites.

- MFRs are twisted magnetic structures that can host cool filament material, hot coronal plasma, and accelerated nonthermal particles.
- They have been observed in **EUV** as hot channels and cavities (*SDO/AIA*) and in **white light** as the classic three-part CME structure (*SOHO/LASCO*).
- Synthetic EUV and WL emission from MHD simulations have successfully reproduced these thermal signatures (e.g., Downs et al. 2011; Lynch et al. 2025)

The gap: The **nonthermal emission** of MFRs produced by accelerated electrons gyrating in the magnetic field has **not yet been modeled** from CME simulations to match radio observations.

Why it matters?

Nonthermal radio emission provides **unique diagnostics** of coronal magnetic field strength and energetic particle distributions within the flux rope that thermal emission cannot provide.

Existing and next-generation radio arrays (*EOVSA, OVRO-LWA, LOFAR, FASR*) can detect microwave and meter-wave emission from CME flux ropes, but their **interpretation requires forward-modeled synthetic radio maps from simulations.**

Key Question: *What are the emission signatures of an erupting flux rope across EUV, WL, and Radio wavelengths?*

Methodology

Simulation: 3D MHD simulation of a breakout CME eruption using the **ARMS** (Adaptively Refined MHD Solver) code (DeVore & Antiochos 2008; Dahlin et al. 2019).

Breakout model:

- A **multipolar magnetic configuration** with a sheared core field.
- Shearing builds free magnetic energy in the core.
- **Breakout reconnection** at the null point above the core removes the overlying flux, triggering eruption.
- The sheared core forms a rising **flux rope** with a trailing flare current sheet. **Flare reconnection** beneath the flux rope builds the post-eruption arcade.

Simulation parameters:

- 3D domain with **adaptive mesh refinement** (AMR)
- Ideal MHD + resistive reconnection at current sheets.
- **Isothermal approximation**: constant coronal temperature throughout the domain.
- Plasma parameters extracted at each time step: density (ρ), velocity (v), magnetic field (B).

Forward modeling

Synthetic EUV (SDO/AIA):

EUV emission depends on electron density squared weighted by the AIA channel temperature response:

$$\mathbf{I}_\lambda = \int_{\mathrm{LOS}} \mathbf{n_e^2}\, \mathbf{R}_\lambda(\mathbf{T})\, \mathbf{dl} \;\Rightarrow\; \mathbf{R}_\lambda(\mathbf{T_0}) \times \int \mathbf{n_e^2}\, \mathbf{dl} \;\Rightarrow\; \mathbf{R}_\lambda(\mathbf{T_0}) \times \mathrm{EM}$$

Synthetic White Light (SOHO/LASCO):

White-light emission arises from **Thomson scattering** of photospheric light by coronal electrons:

$$\mathbf{pB} = \int_{\mathbf{LOS}} \mathbf{n_e}\, \mathbf{G}(\chi)\, \mathbf{dl}$$

Rectilinear Ray-Tracing Algorithm

Works directly on the native spherical grid.
No interpolation to a Cartesian required!

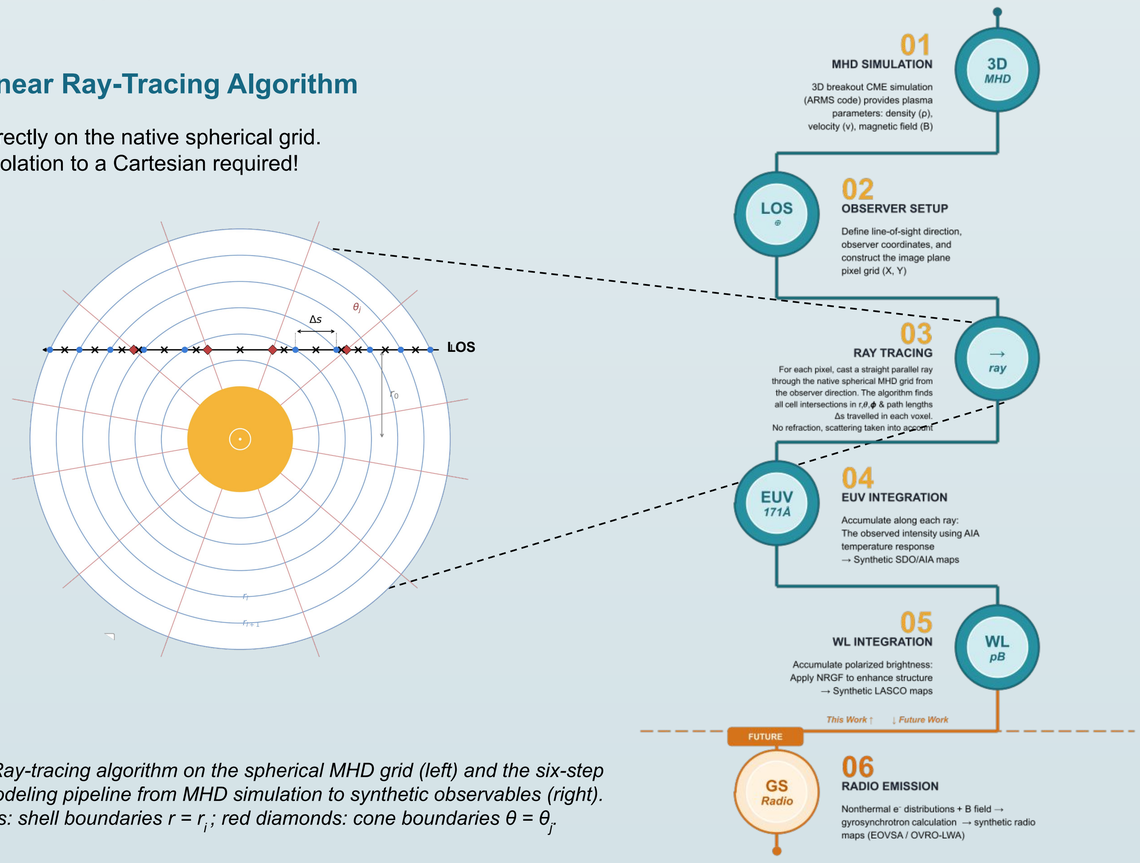


Figure 2. Ray-tracing algorithm on the spherical MHD grid (left) and the six-step forward modeling pipeline from MHD simulation to synthetic observables (right). Blue circles: shell boundaries $r = r_i$; red diamonds: cone boundaries $\theta = \theta_j$.

Results

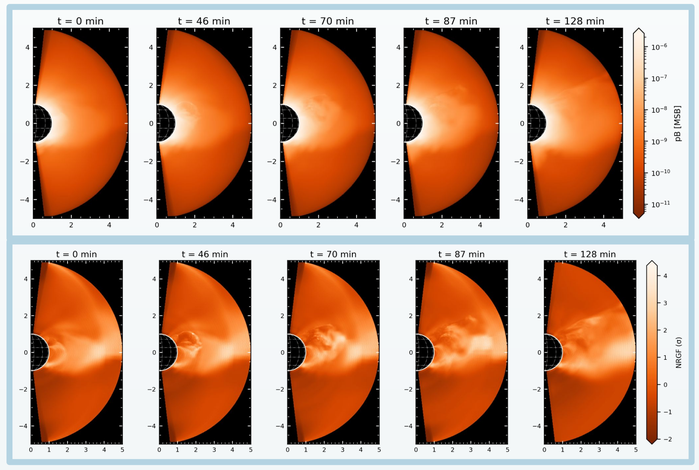


Figure 3. Top: Raw polarized brightness (pB) in MSB (Mean Solar Brightness) from Thomson scattering. Bottom: Normalized Radial Graded Filter (NRGF) processed pB revealing the classic three-part CME structure.

Synthetic WL Emission Maps

t = 0 min: Quiescent corona; radially symmetric pB with no CME signatures.
t = 46 min: Faint density enhancement appears above the limb as the CME enters the coronagraph field of view.
t = 70–87 min: NRGF reveals the classic 3 part CME: bright leading front (compressed sheath), dark cavity (flux rope interior), and bright core (dense entrained material).
t = 128 min: CME front propagates beyond 4$R_\odot$; cavity remains well-defined, indicating the flux rope retains magnetic confinement at large heights.

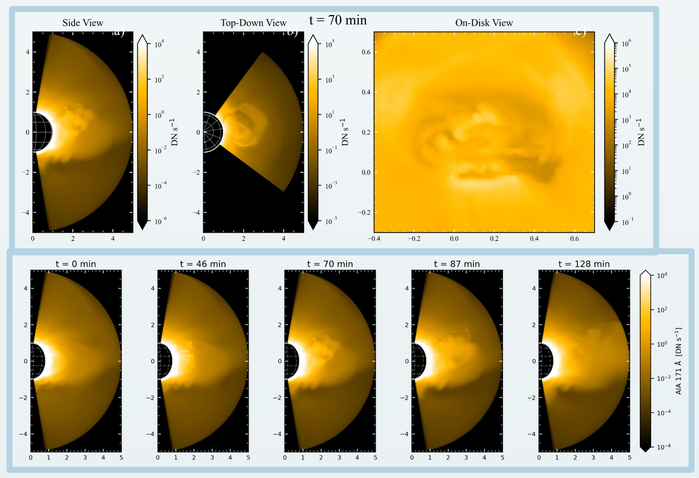


Figure 4. Top: Synthetic AIA 171 Å from three viewing geometries at t = 70 min: (a) limb, (b) north-pole, (c) face-on. Bottom: Temporal evolution of the same from limb view.

Synthetic EUV Emission Maps

Pipeline produces synthetic observables from any viewing angle, enabling multi-spacecraft comparison (SDO, STEREO, Solar Orbiter).

- **t = 0 min:** Pre-eruption sheared arcade with enhanced core density.
- **t = 46 min:** Breakout reconnection destabilizes the field; sheared core begins rising.
- **t = 70–87 min:** Flux rope visible as a density cavity with compressed plasma; trailing current sheet feeds flux into the rope and builds the post-eruption arcade.
- **t = 128 min:** Flux rope expands beyond 3 $R_\odot$; elongated current sheet and well-developed arcade at the base.

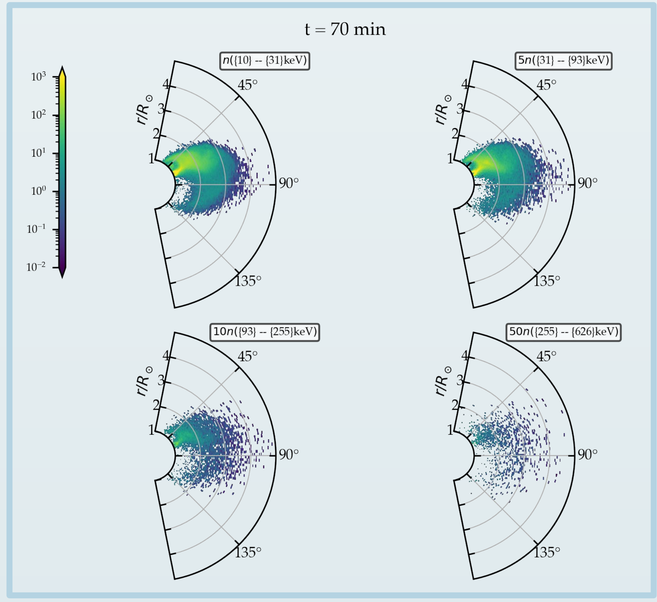


Figure 5. Spatial distribution of non-thermal electrons across four energy ranges at t = 70 min, showing energy-dependent confinement within the flux rope.

Bridging to Radio: Non-Thermal Electron Input

With the **thermal (EUV + WL)** components validated, we now use **nonthermal electron distributions** from test particle simulations (Li et al. 2025) as input to bridge toward **synthetic radio emission.**

- Electron distributions from test particle simulations show clear **energy-dependent structure** inside the flux rope at t = 70 min.
- **High-E electrons** stay **confined** near the **reconnection core**; **low-E electrons disperse** along opening field lines, confirming **reconnection-driven acceleration** and **gyroradius-controlled escape.**
- This maps directly to **radio morphology:** low-E electrons dispersing along open field lines → **extended emission structures** detectable at OVRO-LWA frequencies.

Conclusion

- Developed a rectilinear **ray-tracing forward modeling pipeline** that computes synthetic EUV and white-light emission maps directly from a 3D MHD CME simulation.
- Synthetic EUV maps show the **thermal evolution** of the erupting flux rope across multiple viewing geometries, reproducing features consistent with SDO/AIA observations.
- Synthetic white-light pB maps show the **classic three-part CME morphology** (bright front, dark cavity, bright core) consistent with coronagraph observations.
- Non-thermal electron distributions from test particle modeling reveal **energy-dependent spatial stratification** within the flux rope.
- Established the foundation for a **unified multi-wavelength forward modeling framework**: MHD → thermal observables (EUV + WL) → nonthermal particle distributions → synthetic radio observables.

Future Work

- Extend pipeline to implement **refractive ray-tracing** to account for radio wave bending and scattering in the density-stratified corona. Incorporate test particle electron distributions (Fig. 5) into the thermal flux rope volume to compute **synthetic gyrosynchrotron radio emission**.
- Enable direct comparison with **EOVSA** (1–18 GHz) and **OVRO-LWA** (12–88 MHz) observations of CME flux ropes.
- Conclusively answer where and how the nonthermal electrons are trapped in MFRs.
- Complete the remaining pipeline to generate synthetic radio observables.

This work is supported by NASA and NSF

Watch the Movie

Connect with me